IOPscience iopscience.iop.org

Home Search Collections Journals About Contact us My IOPscience

Non-cubic Er centres in ZnSe studied by electron paramagnetic resonance and optical analysis

This article has been downloaded from IOPscience. Please scroll down to see the full text article.

1995 J. Phys.: Condens. Matter 7 4271

(http://iopscience.iop.org/0953-8984/7/22/010)

View the table of contents for this issue, or go to the journal homepage for more

Download details:
IP Address: 171.66.16.151
The article was downloaded on 12/05/2010 at 21:23

Please note that terms and conditions apply.

J. Phys.: Condens. Matter 7 (1995) 4271–4282. Printed in the UK

Non-cubic Er centres in ZnSe studied by electron paramagnetic resonance and optical analysis

J Dziesiaty†, St Müller†, R Boyn†, Th Buhrow†, A Klimakow† and J Kreissl‡

† Humboldt-Universität zu Berlin, Institut für Physik, Berlin, Germany

‡ Arbeitsgruppe EPR, Institut für Festkörperphyisk der Technischen Universität Berlin, Berlin, Germany

Received 2 February 1995, in final form 14 March 1995

Abstract. EPR and optical (4f–4f photoluminescence and photoluminescence excitation) spectra due to Er centres are studied on bulk ZnSe crystals, which were grown by the high-pressure Bridgman technique and doped with ErF_3 (and partly, in addition, with Li_2CO_3) during crystal growth. Besides the well known, almost isotropic signal with $g = 5.94$, which has been assigned to isolated Er^{3+} on Zn lattice sites, we observe three strongly anisotropic EPR spectra (A, B and B′) which are due to transitions in non-cubic Er^{3+} (spectrum A) and Er^{2+} (spectra B and B′) centres. The symmetry axes of these centres have directions close to ⟨111⟩ (A) and parallel to ⟨110⟩ (B and B′). The angular dependences of the signals are influenced by twinning effects.

In the crystals doped with ErF_3 alone, only a single type of centre, which is obviously identical with the type A EPR centre, manifests itself in photoluminescence. A crystal-field analysis of the corresponding EPR and optical spectra shows that this centre has a Γ_6-type ground level and is characterized by a crystal-field parameter ratio $A_6\langle r^6\rangle/A_4\langle r^4\rangle = -0.22$. We think that this centre is a complex consisting of Er^{3+} on a Zn site and F on a nearest-neighbour interstitial site.

The g-factors found for the EPR signals B and B′ can be explained on the basis of non-Kramers doublet ground levels of Er^{2+} $4f^{12}$ which result from the splitting of cubic Γ_5 triplets due to non-cubic crystal-field components. These two signals are ascribed to Er^{2+} on the two zincblende-type interstitial sites, respectively, each forming a complex with some other kind of atom on its next-nearest-neighbour interstitial site.

A discussion is given of the result that the EPR spectra (unlike the optical spectra) were detected only in the case of Li_2CO_3 codoping.

1. Introduction

There is growing interest in rare-earth (RE)-doped semiconductors because of the possibility of using 4f–4f optical transitions in light-emitting semiconductor devices. This is reflected by a great number of recent studies especially for III–V and Si hosts [1]. These studies as well as earlier work on REs in II–VI material (see the review in [2]) show that the 4f–4f emission efficiency critically depends upon the form in which the RE ions are incorporated into the crystal lattice. General experience emerging from these investigations is that frequently the highest efficiency is obtained if the REs form complexes with other types of defect, introduced, for example, by some kind of codoping. This observation can be easily explained on the basis of earlier studies of the 4f–4f excitation mechanism [3].

On the other hand, detailed investigations of the structure of RE centres in semiconductors using EPR have concentrated on cases of isolated substitutional incorporation, with rather few exceptions dealing with complex centres [2, 4–8]. However, to make progress with the optimization of 4f–4f emission efficiency, work on the latter type of centre, which

0953-8984/95/224271+12$19.50 © 1995 IOP Publishing Ltd

often have lower than cubic symmetry, is necessary. Here it is very important to combine the EPR studies with centre-specific optical analysis to obtain data on both the ground and the excited 4f multiplets.

Our present work refers to low-symmetry Er centres in bulk ZnSe crystals using ErF_3 as the dopant, which was chosen in view of the special interest in optical transitions of Er^{3+} in semiconductors [1], and the positive experience with RE halide doping in the case of ZnS [2, 9]. Part of the studies were made on samples which were additionally codoped with Li, in order to suppress broad-band emission which competed with the 4f–4f emission in the samples doped only with ErF_3. These two kinds of sample will be referred to as Er, F/Li and Er, F type, respectively, in the following. To obtain complementary information on the Er centres, EPR and photoluminescence (PL) as well as 4f–4f photoluminescence excitation (PLE) measurements were made on the same samples.

One of our most remarkable results is that in the case of doping with ErF_3 alone we see a single Er centre active in PL and PLE. This centre is obviously present in high concentrations (see section 4).

2. Samples

The crystals were grown by the high-pressure Bridgman technique. The starting materials were high-purity Merck ZnSe (purity, 99.9999%), Li_2CO_3 (puriss.) and ErF_3 (puriss.), all in the form of powders. The ZnSe was subjected to high-vacuum sublimation, and to annealing in the presence of excess Zn, for additional purification and adjustment of stoichiometry, respectively. The concentration of ErF_3 in the starting material used for the growth of both Er, F and Er, F/Li crystals was 1.5 mol%. Li_2CO_3 was added in the latter case to give a 1:1 molar ratio of Er:Li.

Crystal growth was performed in a tapered cylinder-shaped BN crucible, under 100 atm Ar pressure, at a temperature of 1530 °C which was held for 1 h (homogenization of the melt); this was followed by controlled cooling of the melt. The crystals (length, 20 mm; diameter, 10 mm) exhibited growth twins, as generally found for II–VI crystals obtained from the melt under pressure [10]. These twin planes were parallel to one set of (111) planes and extended completely across the crystals, forming an angle of about 45° with the growth direction. The distances between neighbouring twin planes were irregular, ranging between 0.03 and 5 mm.

Samples of about 1 mm thickness were cleaved from various parts of the ingots, and {110} cleavage faces were used for the excitation and measurement of the PL and as reference planes in the EPR studies. The [001] and $[111]_w$ axes were determined from the angular dependences of the well known Fe^{3+} EPR spectrum [11]. ($[111]_w$ denotes the normal to the (111) twin planes.)

3. Electron paramagnetic resonance spectra

EPR measurements were performed on the Er, F/Li and Er, F samples. Signals due to Er (evidenced by their characteristic hyperfine pattern; $I = \frac{7}{2}$) were only observed in the Er, F/Li case, at $T = 4$ K in the X band (9.4 GHz) and Q band (34 GHz). In all samples the strongest signal (to be referred to as signal C) was nearly isotropic with $g = 5.94$ and a hyperfine splitting constant $A = 0.0212$ T, which could be assigned to the well known spectrum of Er^{3+} on cubic sites in ZnSe having a Γ_7 ground state [4]. The slight anisotropy

of this signal is due to the perturbation by a close-lying Γ_8 level [4]. In our case the g-factor was determined for $B\|[111]_w$, where the regular and the twin-induced spectra coincide and the linewidth has a minimum. It should be noted that signals analogous to C have been detected for Er^{3+} in other II–VI [2] and in III–V [12, 13] materials. Additionally, three strongly anisotropic spectra due to Er were found, namely A, B and B′ (figure 1), which could be described by transitions based on two different spin Hamiltonians (equation (1) for A and equation (2) for B and B′) in twinned ZnSe, characterized by additional symmetry of the spectra, about the $[111]_w$ axis, within the $(110)_w$ plane.

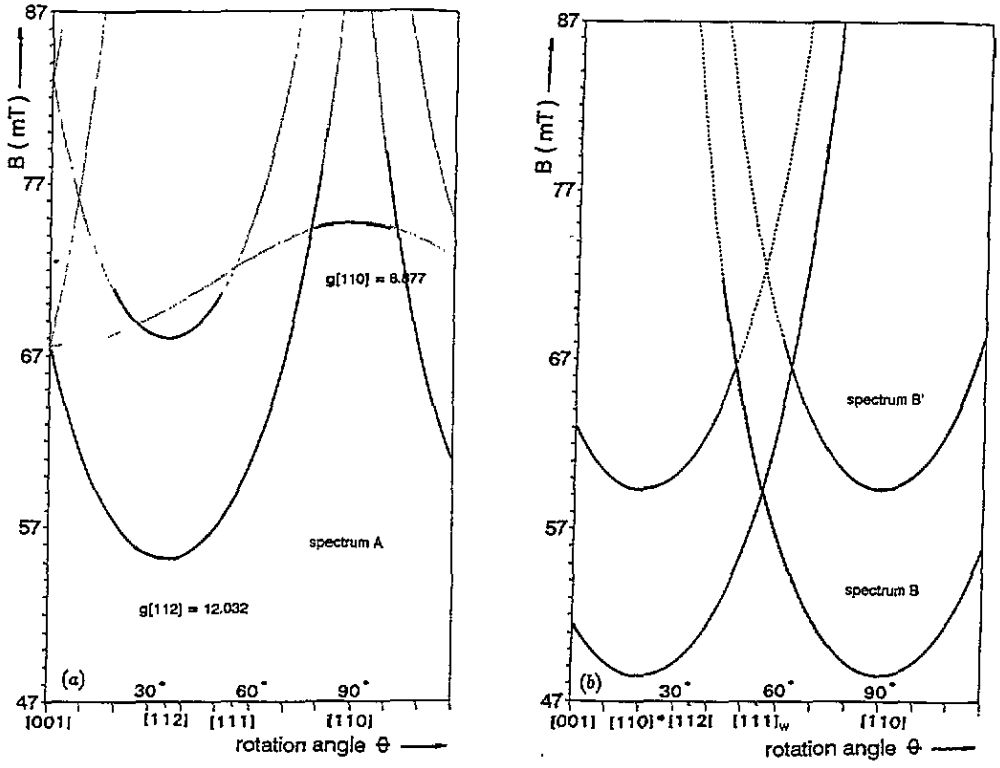

Figure 1. (*a*) EPR angular dependence (X band; $T = 4$ K) for centre A and magnetic field B rotated in a (110) plane not containing the $[111]_w$ axis. [001] is the symmetry axis of the spectrum for the pure cubic case. (*b*) EPR angular dependence (X band; $T = 4$ K) for centres B and B′. Here B was rotated in the $(110)_w$ plane containing the $[111]_w$ axis which, in this case, is the symmetry axis of the spectra. [110] and [110]* refer to the two twin components, respectively, rotated through 60° about the $[111]_w$ axis relative to each other. (Only centres with axes lying in the $(111)_w$ plane are shown.) In both parts of the figure the ranges of experimental points are indicated by broadened curves.

Spectrum A consists of four complexes, each described by a spin Hamiltonian

$$H_{\text{spin}} = \beta \boldsymbol{B} \cdot \mathbf{g} \boldsymbol{S}' \tag{1}$$

with effective spin $S' = \frac{1}{2}$ and rhombic $\mathbf{g}$-tensor (β is the Bohr magneton, and B the magnetic field). Fitting the spectra of figure 1(*a*) to the transitions of (1), one obtains

$$g_1 = g_{(111)} \leqslant 0.57$$

$$g_2 = g_{\langle 110\rangle} = 8.877 \pm 0.001$$

$$g_3 = g_{\langle 112\rangle} = 12.032 \pm 0.001.$$

Hence the **g**-tensor is nearly axial with respect to the $\langle 111\rangle$ directions: $g_\parallel = g_1 \simeq 0$; $g_\perp = \frac{1}{2}(g_1 + g_3) = 10.5$. As discussed in more detail in section 5, spectrum A is related to complexes involving Er^{3+}.

Spectra B and B' can be described by the transitions of a spin Hamiltonian for non-Kramers doublets arising from ions with $S \geqslant 1$, subjected to strong axial splitting [14]:

$$H_{\text{spin}} = g'_\parallel \beta B_z S'_z + \Delta_x S'_x + \Delta_y S'_y + A_\parallel I \cdot S'. \tag{2}$$

This spin Hamiltonian corresponds to rhombically distorted axial complexes, where Δ_x and Δ_y are the splitting factors due to the rhombic field perpendicular to the z symmetry axis, with $g'_\perp = 0$, $g'_\parallel = 2M_S g_\parallel$ and effective spin $S' = \frac{1}{2}$. The Hamiltonian (2) yields transitions at the magnetic field strengths

$$|B| = \frac{\sqrt{(h\nu)^2 - \Delta^2}}{g'_\parallel \beta \cos\Theta} + \frac{M_I A_\parallel}{g'_\parallel \beta \cos\Theta}$$

(Θ is the angle between B and the symmetry axis, and $\Delta^2 = \Delta_x^2 + \Delta_y^2$). From measurements at two microwave frequencies ν (= 9.4 and 34 GHz), one obtains

$$g'_\parallel(\text{B}) = 13.46 \pm 0.01$$

$$g'_\parallel(\text{B}') = 10.95 \pm 0.01 \qquad A_\parallel = 0.0219 \text{ T}$$

$$\Delta = (560 \pm 10) \times 10^{-4} \text{ cm}^{-1}$$

with the z symmetry axis parallel to $\langle 110\rangle$. *In section 5 we shall show that the signals* B and B' are due to centres involving Er^{2+} ions.

4. 4f–4f photoluminescence and photoluminescence excitation spectra

Intrinsic excitation of the PL (excitation through the ZnSe energy bands) was performed by means of the 514.5 nm line of an Ar^+ laser. Three bands of sharp 4f–4f emission lines were studied, which are clearly due to transitions in Er^{3+} ions, namely transitions from the $^4I_{9/2}$, $^4F_{9/2}$ and $^4S_{3/2}$ multiplets to the $^4I_{15/2}$ ground multiplet. (These types of intermultiplet transition were also observed in earlier work on ZnSe:Er, for example [4, 15, 16].) This sharp-line PL was partly superimposed by broad-band emission, especially in the Er, F case; the latter was greatly reduced by the Li coactivation.

The 4f–4f emission was also studied using 4f–4f excitation between individual Stark components instead of the integral excitation considered before. This was done in the $^4I_{15/2} \rightarrow {}^4F_{9/2}$ transition range, with the aid of a dye laser (dye DCM). This is the usual procedure of site-selective (centre-selective) spectroscopy [2]. The remarkable point is that, in the Er, F-type samples, only a single centre was found to be active in luminescence, which is an unusual situation for II–VI systems [2]. This is demonstrated in figure 2, where the $^4F_{9/2} \rightarrow {}^4I_{15/2}$ PL spectrum is compared for integral and selective 4f–4f excitation. The concentration of this centre, which was also seen in 4f–4f absorption, was estimated to

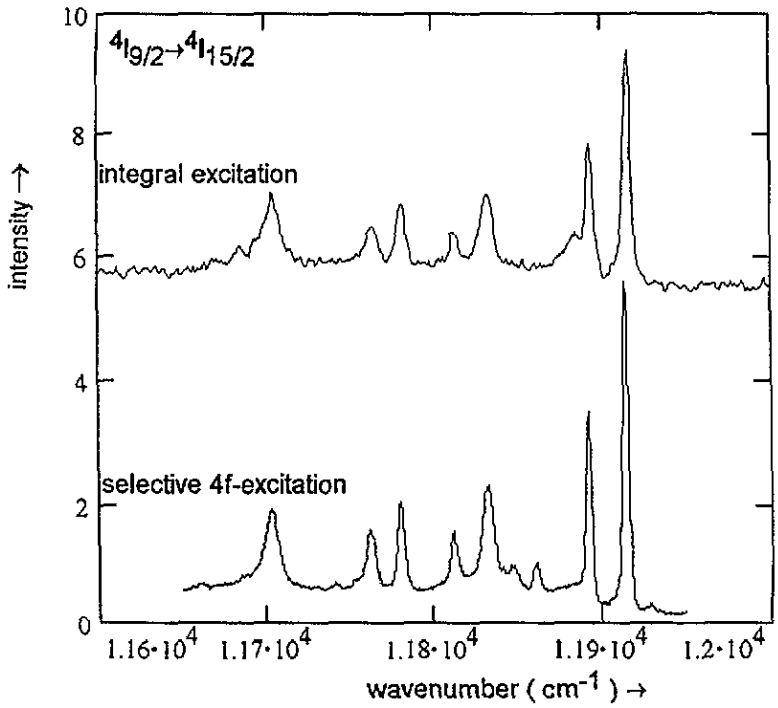

Figure 2. Comparison of the Er^{3+} $^4I_{9/2} \rightarrow {}^4I_{15/2}$ PL spectrum of a ZnSe:Er, F sample for integral (514.5 nm Ar^+ laser) excitation and 'centre-selective' 4f–4f ($^4I_{15/2} \rightarrow {}^4F_{9/2}$, transition 4 (figure 4)) dye laser excitation, demonstrating that in these samples a single centre contributes to the 4f–4f emission ($T = 1.8$ K).

be of the order of 10^{19} cm^{-3}. The single-centre result was checked by looking at various intermultiplet PL transitions under excitation into different $^4F_{9/2}$ Stark components, and by measuring 4f–4f PLE spectra monitoring various combinations of Stark components in the $^4F_{9/2} \rightarrow {}^4I_{15/2}$ and $^4I_{9/2} \rightarrow {}^4I_{15/2}$ PL transitions. Examples are given in figure 3.

From these results, consistent data on the 4f energy spectrum of that centre including the $^4F_{9/2}$ and $^4I_{15/2}$ Stark splittings were derived, and this is depicted in figure 4.

It is immediately evident from these data that we are dealing with a centre of lower than cubic symmetry. For cubic (tetrahedral) symmetry the $^4F_{9/2}$ and $^4I_{15/2}$ levels of the free Er^{3+} ion split into three ($\Gamma_7 + 2\Gamma_8$) and five ($\Gamma_6 + \Gamma_7 + 3\Gamma_8$) components, respectively [17]. Instead, in our experimental spectra we see five and eight components respectively. These are exactly the numbers of components expected for $J = \frac{9}{2}$ and $J = \frac{15}{2}$ levels in a non-cubic centre, where each of the cubic Γ_8 levels is additionally split into two components. In section 5 we shall argue that the centres under discussion are identical with the type A centres detected in the EPR spectra.

For the Er, F/Li samples we see other types of Er^{3+} centre in addition to the centres occurring in the Er, F case. This is shown in figure 5. The additional centres have not been analysed in detail so far by optical spectroscopy.

5. Discussion of the types of centre

As a starting point of our discussion we shall use the level diagrams of Lea, Leask and Wolf (LLW) [17] referring to cubic symmetry. For the non-cubic centres this procedure

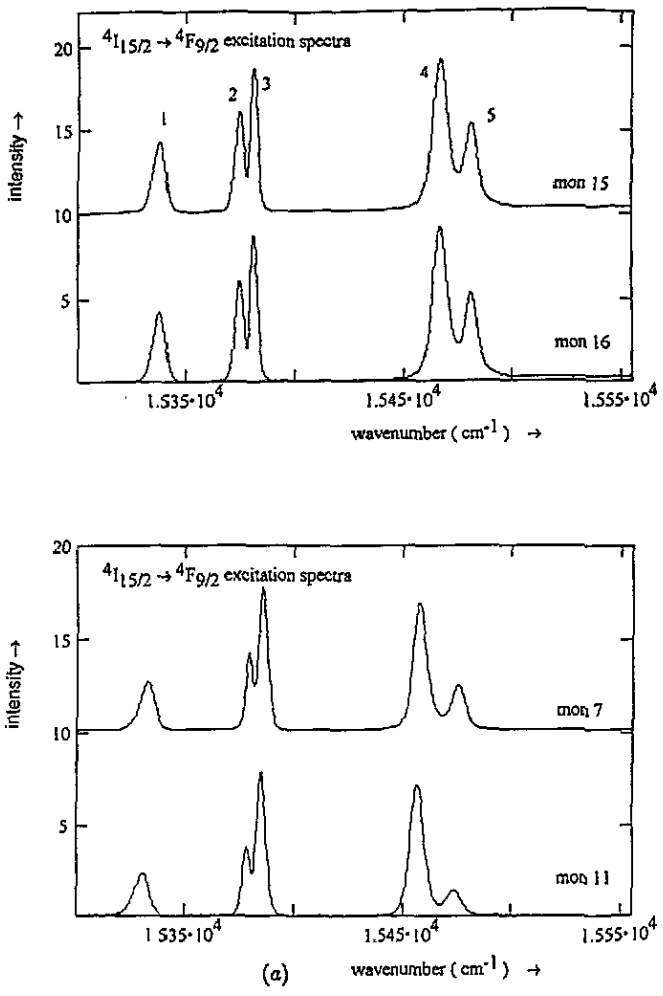

Figure 3. (*a*) 4f–4f PLE spectra and (*b*) 4f–4f PL spectra under 4f–4f excitation of the Er^{3+} centres (A) occurring in the ZnSe:Er, F samples. The numbers on the lines refer to the labelling of transitions in figure 4. For each spectrum the transition monitored (mon) or used for excitation (exc) is indicated. Phonon-assisted transitions are denoted by PA ($T = 1.8$ K).

(which has been employed in earlier work on similar systems [5, 6]) will be justified if the non-cubic crystal-field components are not too strong. In this case we can also expect that the **g**-tensor components $g_\parallel$ and $g_\perp$ of axial centres are related to the corresponding 'cubic' values g_c through $g_c = \frac{1}{3}(g_\parallel + 2g_\perp)$.

For centres involving Er^{3+} the EPR data refer to the lowest $^4I_{15/2}$ crystal-field component (figure 6). If this component is one of the Kramers doublets Γ_6 and Γ_7, we have

$$g_c = 2g_L(\Gamma_i|J_z|\Gamma_i) \qquad i = 6 \text{ or } 7$$

since the Γ_6 and Γ_7 wavefunctions and, hence, the matrix elements of the angular moment component J_z are determined by symmetry alone [17]. Here g_L is the Landé splitting factor, which has the value $\frac{6}{5}$ for a 'pure' $^4I_{15/2}$ state. Thus one obtains $g_c = 6.8$ and $g_c = 6.0$ for

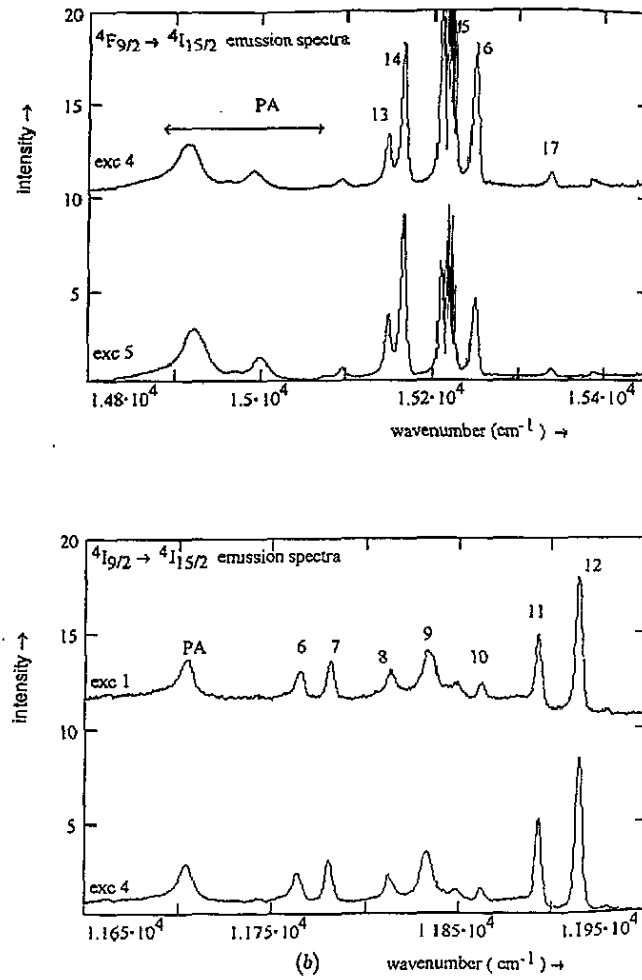

Figure 3. (Continued)

Γ_6 and Γ_7 states, respectively. In the following we discuss the individual centres, starting from the respective EPR signals.

5.1. Centre C

Because centre C has a g-value only slightly less than 6.0 it is concluded that one is dealing with a Γ_7 ground level. According to figure 6, this implies that $W > 0$ and $-1 < x < -0.46$ for the parameters introduced by LLW [17]. The detailed analysis of this signal given in [4] leads to $x = -0.71$. In agreement with [4] we assign this signal to (isolated) Er^{3+} ions on Zn sites. We also find a slight anisotropy of spectrum C originating from a close-lying Γ_8 level. Compared with [4], this angular dependence is modified by the presence of twinning in our case.

5.2. Centre A

For this Er^{3+} centre the averaged g-value $\frac{1}{3}(g_\parallel + 2g_\perp)$ is found to be 6.97 (cf. section 3).

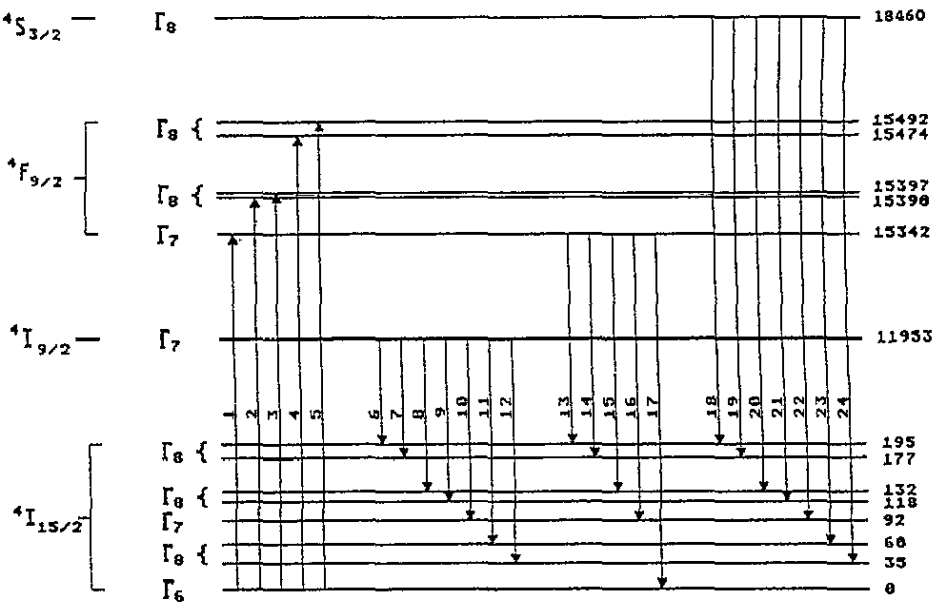

Figure 4. 4f energy spectrum of the Er^{3+} centre manifesting itself in the PL and PLE spectra, including the transitions observed in experiment and the assignments to 'cubic' crystal-field components (energies in reciprocal centimetres).

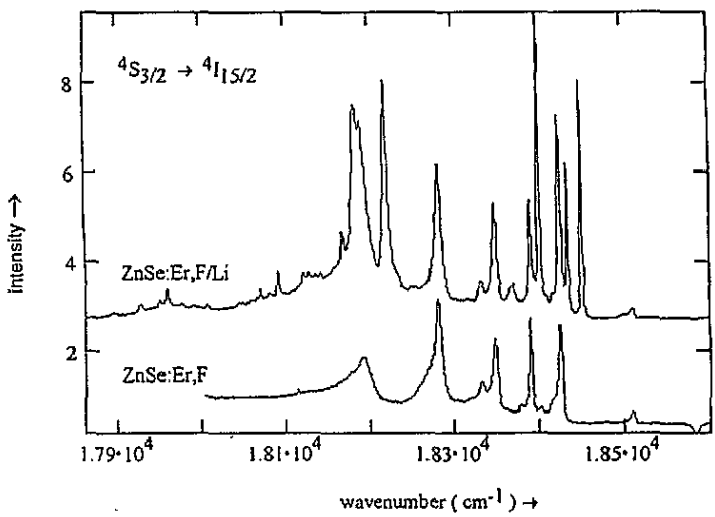

Figure 5. Comparison of the PL spectra of a ZnSe:Er, F and a ZnSe:Er, F/Li sample in the range of the Er^{3+} $^4S_{3/2} \rightarrow {}^4I_{15/2}$ transitions measured with integral (514.5 nm Ar^+ laser) excitation (T = 1.8 K). In the ZnSe:Er,Li spectrum the sharp lines between 18 230 and 18 500 cm^{-1} are assigned to the pure electronic transitions 18–24 (figure 4), while the broad line about 18 190 cm^{-1} is probably due to phonon-assisted transitions.

This result, together with the optical data to be discussed below, indicates that we are concerned with a Γ_6 'cubic parent' ground level, which implies that $-0.4 < x < +0.6$,

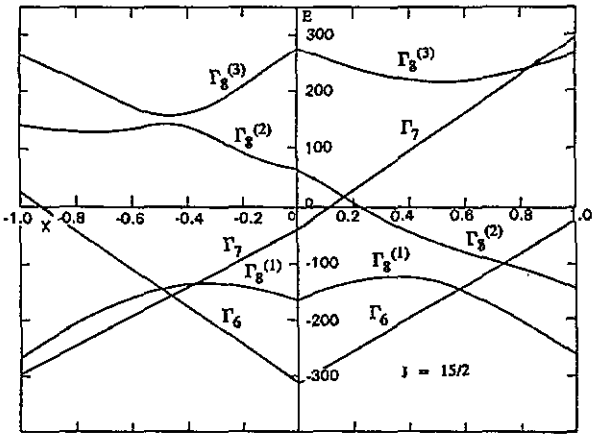

Figure 6. LLW diagram [17] describing the splitting of a $J = 15/2$ level in a crystal field of cubic (tetrahedral) symmetry.

$W > 0$ (figure 6).

The results of the optical studies (figures 2–4) can also be interpreted on the basis of a non-cubic centre having a Γ_6 parent ground level. Looking at the $^4I_{15/2}$ Stark components (figure 4) we see that there are three 'doublets' having a relatively small separation of components (indicated by curly brackets). It seems natural to assign these doublets to Γ_8 levels split by the non-cubic perturbation. So, for $x \simeq -0.3$ we get an order of parent states consistent with figure 4, in which the corresponding assignment of the $^4I_{15/2}$ components is indicated. This x-value implies that $\lambda \equiv A_6\langle r^6\rangle / A_4\langle r^4\rangle = -0.22$ for the ratio of the cubic crystal-field parameters.

Similar arguments can be applied to the $^4F_{9/2}$ levels observed optically, where the assignment to Γ_8 doublets is still more suggestive (figures 3 and 4). Using the above λ-value and Stevens parameters given in [18], we get $x = 0.7$, $W < 0$, for the cubic Stark splitting of $^4F_{9/2}$, which yields the level order Γ_8–Γ_7–Γ_8, while the situation observed in experiment (Γ_7–Γ_8–Γ_8 (figure 4)) requires $x \simeq 0.87$, $W < 0$. We feel that the inclusion of non-cubic crystal-field terms can remove this small discrepancy. Unfortunately, owing to the large number of crystal-field parameters in the non-cubic case, a more quantitative discussion cannot be given.

These results indicate that the centre observed in the PL and PLE spectra is identical with centre A seen in EPR.

We think that the most plausible model for centre A is a complex consisting of an Er^{3+} ion on a Zn site and a negatively charged F ion on a nearest-neighbour (NN) interstitial site (interstitial site surrounded by three Zn ions and the Er ion). The symmetry axes of such complexes, with the ions in ideal positions, are parallel to ⟨111⟩. Small distortions of these high-symmetry configurations such as found for other deep-impurity systems [19] should be responsible for the rhombic character of the **g**-tensor. For a complex of that kind, $g_\parallel$ is expected [20] to be smaller than $g_\perp$, in agreement with our experimental result.

The present model is supported by the fact that the signs of the x- and W-values coincide with those found for the isolated Er^{3+} on Zn sites (centre C). This means that in the quasi-cubic framework we have $A_4\langle r^4\rangle < 0$ and $A_6\langle r^6\rangle > 0$ also for centre A. On the other hand, for the parameter λ introduced above, we have a value of much smaller magnitude in case C ($\lambda = -0.037$ from the data [4]). The increase in $|\lambda|$ obtained when adding an F ion to

the centre is consistent with the experience from work on non-cubic rare-earth centres in ionic hosts [21] which indicates an appreciable decrease in $|A_4\langle r^4\rangle|$ and increase in $|A_6\langle r^6\rangle|$ occurring owing to an axial perturbation.

A situation analogous to that for centre A has been met in EPR studies of the system ZnTe:Er, P [6] where Er^{3+} centres with ⟨111⟩ symmetry axes and Γ_6-like ground levels have been observed. These centres have been identified as Er on Zn sites associated with P on NN Te sites. Thus these centres differ from our A-centre assignment in that the disturbed NN chalcogen tetrahedron instead of the NN interstitial site tetrahedron is involved. The presence of a Γ_6-like ground level for the Er–P centre implies similar x- and λ-values as in our case, with an analogous physical reason for their deviation from those of the isolated Er_{Zn} Γ_7-type centre.

5.3. Centres B and B′

Spectra described by a spin Hamiltonian of the form (2) with $g_\perp = 0$ may be observed in the case of non-Kramers doublets, as arising from RE ions with integral J [14]. Therefore we assume that spectra B and B′ are due to near-axial complexes of Er^{2+}.

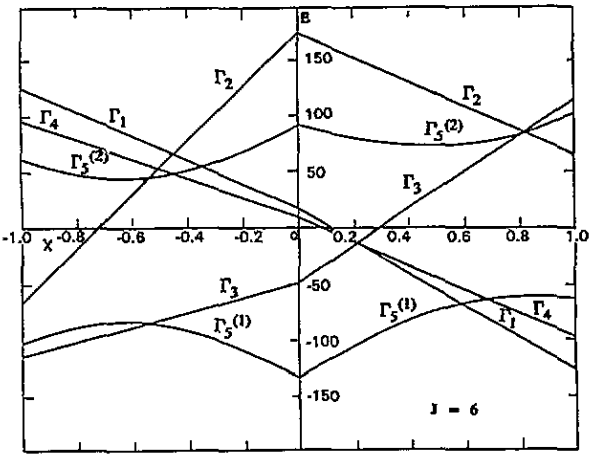

Figure 7. LLW *diagram [17] describing the splitting of a $J = 6$ level in a crystal field of cubic* symmetry.

The LLW diagram (figure 7) shows that for $J = 6$ there are three triplets Γ_4, $\Gamma_5^{(1)}$ and $\Gamma_5^{(2)}$ (effective spin $S = 1$), each splitting into a singlet and a doublet due to an axial perturbation.

An additional rhombic crystal-field component V_2^2 has matrix elements between the $M_S = 0$ and $M_S = \pm 1$ states, giving an allowed transition between the latter, with $g'_\parallel = 4g_L\langle\Gamma_5|J_z|\Gamma_5\rangle$, if the oscillatory magnetic field at resonance has a component along the z axis [14]. From the $g'_\parallel$-values found experimentally (section 3) we get

$$\langle\Gamma_5|J_z|\Gamma_5\rangle_B = 2.89 \qquad \langle\Gamma_5|J_z|\Gamma_5\rangle_{B'} = 2.35.$$

On the basis of the $J = 6$ wavefunctions given by LLW [17], one obtains such values for a $\Gamma_5^{(1)}$ ground-state triplet ($W > 0$) with $x = 0.5$ and $x = -0.45$, respectively. The case $W > 0$, $x > 0$, may be realized for Er^{2+} on an interstitial site with four positively charged

nearest-neighbour ions, whereas the case $W > 0$, $x < 0$, should occur for interstitials coordinated by four negatively charged ions. This result is based on the structure of the two types of zincblende interstitial site, for which the NN ionic tetrahedron and the next-nearest-neighbour (NNN) ionic octahedron are thought to dominate the crystal field [2], and on Tm^{3+} Stevens parameters, which should agree with those of Er^{2+} with respect to the signs. It may be assumed, therefore, that the Er^{2+} ions are on both types of interstitial site, each strongly disturbed by axial fields in ⟨110⟩ directions. These fields could be due to association with atoms on NNN interstitial sites, i.e. interstitial sites of the same type as occupied by the Er^{2+} in each of the two cases. In addition to F ions, partner ions related to the Li_2CO_3 codoping may be involved in the centres B and B′. The latter variant would explain why the respective EPR signals were not found in the Er, F samples.

6. Concluding discussion

Four signals have been observed in our EPR studies.

(1) Signal C, which is already known from earlier work [4], is very probably due to isolated Er^{3+} on Zn sites.

(2) Signal A is assigned to Er^{3+} on Zn sites associated with F on a NN interstitial site (interstitial site surrounded by three Zn atoms and the Er).

(3) Signal B and (4) signal B′ are attributed to complexes which consist of Er^{2+} on interstitial sites surrounded by four NN Zn and four NN Se atoms, respectively, and a partner atom on the NNN interstitial site (interstitial site of the same type in each case).

Centre A has been detected also in our optical measurements, which have given information on its 4f energy spectrum.

Our results suggest the presence of interstitial Er in the 2+ state, which obviously implies that the respective ground levels are below the conduction band edge. A trend toward deep-lying 2+ levels occurring at the end of the lanthanide series has been predicted for substitutional site occupation [22, 23], and this is consistent with available experimental data [24]. For RE interstitials there have been, so far, no theoretical discussions concerning this point; however, recent experimental work on ZnS:Tm [7] establishes the presence of interstitials in the 2+ state for Tm, which is adjacent to Er in the periodic table. On the other hand, it should be emphasized that the position of RE ground levels relative to the energy bands should significantly depend on the host material as well as on the structure and the constituents of complex centres. In particular, we think that the observation of Er^{3+} interstitial complex centres in ZnSe [4] and ZnTe [6] is consistent with our results concerning centres B and B′.

Let us finally comment on the fact that EPR signals were observed only in the case of Li_2CO_3 codoping. For centres B, B′ and C the probable reason is that the respective concentrations were too low in the Er, F samples. This is not surprising in case C, since for isolated substitutional centres it has been found earlier [6] that acceptor codoping is necessary for the incorporation of significant concentrations. On the other hand, centres B and B′ may be absent in the Er, F cases, because codopant atoms are likely to be constituents of these complexes.

A real puzzle is the absence of type A EPR signals in the Er, F samples, as confronted with the result that the corresponding optical spectra were found with and without Li_2CO_3 codoping, the latter giving evidence of high concentrations of the type A centres. The only possible way of interpretation seems to be a significant broadening of EPR lines in

the Er, F case due to relatively short spin–lattice relaxation times (smaller than 10^{-6} s). Such a shortening could arise from the interaction of 4f spins with electronic states outside the 4f shell considered, which have energies close to the ZnSe conduction band (possibly donor-type states). Li codoping would compensate (empty) these states, thus reducing the linewidth and enabling the EPR signals to be observed. If the overlap of those orbitals with the 4f shell is insignificant, the optical spectra should agree in the two cases as found in experiment (figure 5).

Acknowledgments

We are greatly indebted to U W Pohl for enabling the high-pressure Bridgman growth to be performed in his laboratory, and to D Wruck for critically reading the manuscript.

References

[1] 1993 *Proc. Symp. on Rare Earth Doped Semiconductors (San Francisco, CA, April 1993) (Mater. Res. Soc. Symp. Proc. 301)* (Pittsburgh, PA: Materials Research Society)
[2] Boyn R 1988 *Phys. Status Solidi* b **148** 11
[3] Zimmermann H and Boyn R 1986 *Phys. Status Solidi* b **135** 379
[4] Kingsley J D and Aven M 1967 *Phys. Rev.* **155** 235
[5] Watts R K and Holton W C 1968 *Phys. Rev.* **173** 417
[6] Crowder B L, Title R S and Pettit G D 1969 *Phys. Rev.* **181** 567
[7] Müller St and Dziesiaty J 1994 *Phys. Status Solidi* b **184** 483
[8] Gennaro A M, Martins G B, Rettori C, Barberis G E and An C Y 1993 *Proc. Symp. on Rare Earth Doped Semiconductors (San Francisco, CA, April 1993) (Mater. Res. Soc. Symp. Proc. 301)* (Pittsburgh, PA: Materials Research Society) p 213
[9] Kato A, Katayama M, Mizutani A, Hattori Y and Ito N 1994 *J. Appl. Phys.* **76** 3206
[10] Terashima K and Takena M 1991 *J. Cryst. Growth* **110** 623
[11] Dieleman J 1965 *Philips Res. Rep.* **20** 206
[12] Bäumler M, Schneider J, Köhl F and Tomzig E 1987 *J. Phys. C: Solid State Phys.* **20** L963
[13] Masterov V F, Shtelmakh K F and Zakharenkov L F 1987 *Sov. Phys.–Semicond.* **21** 223
[14] Abragam A and Bleaney B 1970 *Electron Paramagnetic Resonance of Transition Ions* (Oxford: Clarendon)
[15] Brown M R, Cox A F J, Shand W A and Williams J M 1972 *J. Phys. C: Solid State Phys.* **5** 502
[16] Abolhassani N and Bryant F J 1987 *J. Phys. C: Solid State Phys.* **20** 207
[17] Lea K R, Leask M J M and Wolf W P 1962 *J. Phys. Chem. Solids* **23** 1381
[18] Dieke G H 1969 *Spectra and Energy Levels of Rare Earth Ions in Crystals* (New York: Wiley)
[19] Pantelides S T 1992 *Deep Centers in Semiconductors* ed S T Pantelides (New York: Gordon and Breach)
[20] Ranon U and Low W 1963 *Phys. Rev.* **132** 1609
[21] Baker J M and Blake W B J 1970 *Proc. R. Soc.* A **316** 63
[22] Delerue C and Lannoo M 1991 *Phys. Rev. Lett.* **67** 3006
[23] Swiatek K, Suchocki A and Godlewski M 1990 *Appl. Phys. Lett.* **56** 195
[24] Przybylinska H, Swiatek K, Stapor A and Godlewski M 1989 *Phys. Rev.* B **40** 1748